2014-12

Effect of Dynamical Instability on Timing Jitter in Passively Mode-Locked Quantum-Dot Lasers

UTD AUTHOR(S): Dmitry I. Rachinskii

Pimenov, A., T. Habruseva, D. Rachinskii, S. P. Hegarty, et al. 2014. "Effect of dynamical instability on timing jitter in passively mode-locked quantum-dot lasers." Optics Letters 39(24): doi:10.1364/OL.39.006815.

Effect of dynamical instability on timing jitter in passively mode-locked quantum-dot lasers

A. Pimenov,[1,*] T. Habruseva,[2,3,4] D. Rachinskii,[5,6] S. P. Hegarty,[2,3] G. Huyet,[2,3,7] and A. G. Vladimirov[1,8]

[1]*Weierstrass Institute, Mohrenstrasse 39, D-10117 Berlin, Germany*

[2]*Centre for Advanced Photonics and Process Analysis, CIT, Cork, Ireland*

[3]*Tyndall National Institute, University College Cork, Cork, Ireland*

[4]*Aston University, Aston Triangle, B4 7ET, Birmingham, UK*

[5]*Department of Mathematical Sciences, The University of Texas at Dallas, USA*

[6]*Department of Applied Mathematics, University College Cork, Ireland*

[7]*National Research University of Information Technologies, Mechanics and Optics, 199034 St Petersburg, Russia*

[8]*Lobachevsky University of Nizhny Novgorod, Russia*

**Corresponding author: pimenov@wias-berlin.de*

Received September 22, 2014; revised October 27, 2014; accepted October 31, 2014;
posted November 3, 2014 (Doc. ID 223432); published December 8, 2014

We study the effect of noise on the dynamics of passively mode-locked semiconductor lasers both experimentally and theoretically. A method combining analytical and numerical approaches for estimation of pulse timing jitter is proposed. We investigate how the presence of dynamical features such as wavelength bistability in a quantum-dot laser affects timing jitter. © 2014 Optical Society of America

OCIS codes: (140.4050) Mode-locked lasers; (140.5960) Semiconductor lasers; (190.1450) Bistability; (230.5590) Quantum-well, -wire and -dot devices; (250.5960) Semiconductor lasers.
http://dx.doi.org/10.1364/OL.39.006815

Semiconductor mode-locked lasers received much attention in the last decade due to their multiple potential applications including high-speed optical telecommunications and clocking [1,2]. Pulses generated by these lasers are affected by noise due to spontaneous emission and other factors such as cavity optical-length fluctuations. In particular, their temporal positions in a pulse train deviate from those of the perfectly periodic output. This phenomenon called timing jitter limits the performance of mode-locked devices [3]. Passive mode-locking is an attractive technique for periodic short-pulse generation due to simplicity of implementation and handling as compared to other techniques such as hybrid or active mode-locking. However, in the absence of external reference clock, passively mode-locked lasers exhibit relatively large pulse timing jitter [4]. Bistable semiconductor lasers can be used as a basic element for optical switches [5,6] where the timing jitter can play a significant role as well.

Analytical approach to the study of the influence of noise on mode-locked pulses propagating in the laser cavity was developed by Haus and Mecozzi [7]. Later this technique was extended to include the effects of carrier density in semiconductor lasers [8]. However, many simplifications involved in the analysis of Refs. [7,8] limit its applicability to modeling dynamics of semiconductor lasers under the influence of noise. In the last two decades, extensive numerical simulations of traveling wave [9,10] and delay differential [11] models were performed to study timing jitter for different laser device configurations. In this report using a delay differential equation (DDE) model of a two-section passively mode-locked semiconductor laser [12], we study the effect of noise on the characteristics of fundamental mode-locked regime and develop a semianalytical method for estimation of pulse timing jitter, which helps us to avoid high computational cost of a purely numerical approach. With the help of DDE-BIFTOOL [13], we perform numerical bifurcation analysis of the model and demonstrate the existence of bistability between two fundamental mode-locked regimes with different pulse repetition frequencies. It was demonstrated experimentally that at low currents, the pulse timing jitter decreases monotonously with the increase of the injection current [9], whereas at higher currents, it may increase with the current [14]. By varying the injection current applied to the gain section, we show both experimentally and theoretically that the pulse timing jitter can exhibit sharp peaks in the vicinity of a bifurcation point of the mode-locked regime. We study how the presence of dynamical instability can induce a dramatic increase of the timing jitter of a mode-locked regime. Furthermore, we demonstrate an abrupt drop of the timing jitter level after a transition between two branches of fundamental mode-locked regime. The observed dependencies of the jitter on the injection current can be considered as general patterns for the semiconductor lasers with transitions between two bistable mode-locked regimes. We find both theoretically and experimentally that, in some quantum-dot laser samples, timing jitter can be reduced with the additional increase of the injection current, which also shifts the mode-locking frequency.

We consider a DDE model of a two-section passively mode-locked semiconductor laser introduced in [12]:

$$\partial_t A + (\gamma + i\Omega)A = \gamma\sqrt{\kappa}\exp\left\{\frac{1-i\alpha_g}{2}G(t-\tau) - \frac{1-i\alpha_q}{2}Q(t-\tau) + i\varphi\right\}A(t-\tau) + \xi\eta(t), \quad (1)$$

$$\partial_t G = g_0 - \gamma_g G - (e^G - 1)|A|^2, \tag{2}$$

$$\partial_t Q = q_0 - \gamma_q Q - s(1 - e^{-Q})e^G|A|^2, \tag{3}$$

where $A(t)$ is the electric field envelope, $G(t)$ and $Q(t)$ are saturable gain and loss introduced by the gain and absorber sections correspondingly, τ is the cold cavity round-trip time, g_0 and q_0 are unsaturated gain (pump) and absorption parameters, $\alpha_{g,q}$ are linewidth enhancement factors in the gain and absorber sections, s is a saturation parameter, $\gamma_{g,q}$ are carrier relaxation rates, γ is the spectral filtering bandwidth, κ is the linear attenuation factor per cavity round trip, and $\eta(t)$ is δ-correlated Langevin noise of amplitude ξ [11]:

$$\eta(t) = \eta_1(t) + i\eta_2(t), \qquad \langle \eta_i(t) \rangle = 0,$$
$$\langle \eta_i(t)\eta_j(t') \rangle = \delta_{i,j}\delta(t - t').$$

We denote by $\psi(t) = (\mathrm{Re}\, A, \mathrm{Im}\, A, G, Q)^T$ a real-valued solution of (1). Direct numerical estimation of pulse timing jitter in DDE model (1)–(3) requires simulation of millions of cavity round trips [10,11]. As it was shown by Haus and coauthors within the framework of the Haus master equation [7,8], the small noise term can be treated as a perturbation to a time-periodic system, and the timing jitter can be estimated by analyzing the properties of the model equation in the vicinity of the mode-locked solution on a single period. In this report following this idea, we develop a semi-analytical method for estimation of pulse timing jitter σ_{var} in DDE model (1)–(3), which relaxes a restriction of the Haus master equation regarding small gain and loss per cavity round trip [12].

We consider a locally stable fundamental mode-locked T_0-periodic solution $\psi_0(t) = (\mathrm{Re}\, A_0, \mathrm{Im}\, A_0, G_0, Q_0)^T$ of system (1)–(3) with $\xi = 0$. Assuming $\xi \ll 1$, we study the local dynamics of trajectories of Eqs. (1)–(3) near the periodic solution using linearization of the system around this solution. Substituting $\psi(t) = \psi_0(t) + \delta\psi(t)$ into (1)–(3) and supposing that $|\delta\psi| \ll 1$ we obtain

$$-\frac{d}{dt}\delta\psi(t) + B(t)\delta\psi(t) + C(t-\tau)\delta\psi(t-\tau) + w(t) = 0, \tag{4}$$

where B and C are the Jacobi matrices of the linearization [15], $w(t) = \xi(\mathrm{Re}\,\eta(t), \mathrm{Im}\,\eta(t), 0, 0)^T$. The homogeneous system (4) with $w(t) \equiv 0$ has two linearly independent periodic solutions, the so-called neutral modes $\delta\psi_{0\theta} = d\psi_0(t)/dt$ and $\delta\psi_{0\varphi} = (-\mathrm{Im}\, A_0, \mathrm{Re}\, A_0, 0, 0)^T$, which correspond to the time shift $\psi_0(t) \to \psi_0(t + t_0)$ and phase shift $A_0(t) \to e^{i\nu}A_0(t)$ symmetry of the system (1)–(3), respectively.

Let $\delta\psi$ be a solution of homogeneous problem (4) with $w(t) \equiv 0$ and a row vector $\delta\psi^\dagger(t) = (\delta\psi_1^\dagger, \delta\psi_2^\dagger, \delta\psi_3^\dagger, \delta\psi_4^\dagger)$ be a solution of the adjoint problem

$$\frac{d}{dt}\delta\psi^\dagger(t) + \delta\psi^\dagger(t)B(t) + \delta\psi^\dagger(t+\tau)C(t) = 0. \tag{5}$$

For solutions $\delta\psi$ of (4) and $\delta\psi^\dagger$ of (5), we consider the following bilinear form [16,17]:

$$[\delta\psi^\dagger, \delta\psi](t) = \delta\psi^\dagger(t)\delta\psi(t) + \int_{-\tau}^{0} \delta\psi^\dagger(t+\theta+\tau)C(t+\theta)\delta\psi(t+\theta)\mathrm{d}\theta. \tag{6}$$

Adjoint periodic eigenfunctions $\delta\psi_{0\theta}^\dagger$ and $\delta\psi_{0\varphi}^\dagger$ (neutral modes of (5)) are T_0-periodic and satisfy biorthogonality conditions $[\delta\psi_{0j}^\dagger, \delta\psi_{0k}] = \delta_{jk}$, where $j,k = \{\theta, \varphi\}$. Timing jitter σ_{var} is given by the variance of the projection of the Langevin perturbation term $w(t)$ on the neutral eigenfunction $\delta\psi_{0\theta}$ corresponding to the time shift invariance of the model equations. Applying the variation of constants formula [17] to Eq. (4), we obtain

$$\sigma_{\mathrm{var}}^2 = \xi^2 \int_0^{T_0} \{[\delta\psi_{0\theta,1}^\dagger(s)]^2 + [\delta\psi_{0\theta,2}^\dagger(s)]^2\}\mathrm{d}s. \tag{7}$$

The experiments were performed with two-section monolithic quantum-dot mode-locked devices. The active region consisted of 15 layers of InAs quantum-dots grown on GaAs substrate at Innolume GmbH; for details of the layer structure see [18]. The devices were cleaved with no coatings applied to the facets and mounted on a temperature controlled stage. We used a set of lasers with different absorber lengths in the experiments.

Pulse timing jitter fluctuations were measured via the integration of the normalized power spectral density (PSD), $L_{\mathrm{RF}}(f)$, over a certain range [19,20]:

$$\sigma^i(f_1, f_2) = \frac{T_r}{2\pi}\sqrt{2\int_{f_1}^{f_2} L_{\mathrm{RF}}(f)\mathrm{d}f}, \tag{8}$$

where σ^i is an integrated timing jitter, f_1 and f_2 are the integration limits, and T_r is the pulse train period. The single sideband PSD was measured from the output radio-frequency (RF) spectrum using an Advantest electronic spectrum analyzer (ESA), a fast photodetector, and an amplifier. The normalized PSD is given by the expression:

$$L_{\mathrm{RF}}(f) = \frac{S_{\mathrm{RF}}(f)}{\mathrm{RBW} \times S_t}, \tag{9}$$

where S_t is the peak signal power, RBW is the resolution bandwidth of the ESA, and $S_{\mathrm{RF}}(f)$ is PSD. The single sideband PSD was integrated over the range of 20 kHz–80 MHz as shown in Fig. 1(a), from both sides.

Figure 1(b) shows measured timing jitter for the lasers P_1 (red) and P_2 (black) with 17% and 12% absorber sections and –1.0 V and –2.0 V reverse bias, respectively, as a function of gain current. For the laser P_1, the jitter decreases with the gain current, while for the laser P_2, the integrated jitter behavior was nonmonotonic with values ranging from 11 to 23 ps.

Figure 2(a) shows measured RF spectrum evolution versus gain current for the laser P_3 with 20% absorber section and –4.0 V reverse bias. The transition between two mode-locked regimes can be seen at the gain current of around 209 mA with shifts of the repetition rate and optical spectrum (to longer wavelengths by 10 nm) and decrease of jitter (from 3 ps for 209 mA to 0.6 ps for 210 mA). Examples of the RF spectra at the transition

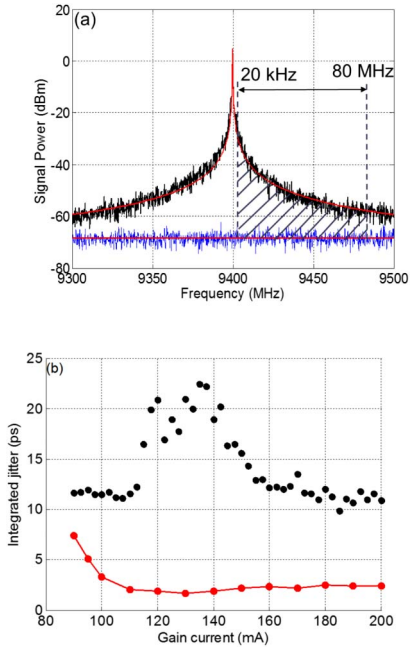

Fig. 1. (a) Integration of timing jitter. Measured RF signal (black, top curve), Lorentzian fit (red), and the noise floor (blue, bottom curve), laser P_2. (b) Integrated timing jitter for lasers P_1 (red, bottom curve) and P_2 (black, top curve) versus gain.

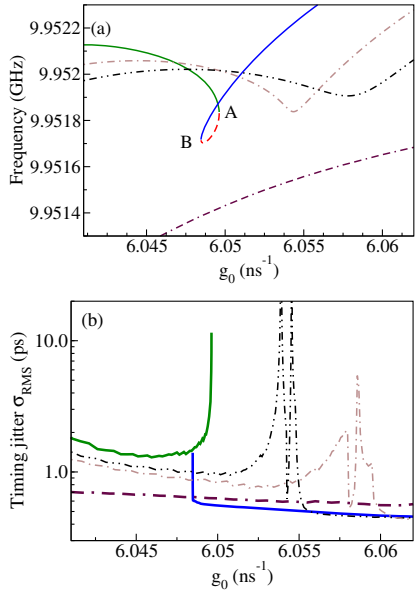

Fig. 3. Branches of fundamental ML regime (a) and corresponding timing jitter (b) for $\alpha_g = 3.7$ (dashed–dashed–dotted), $\alpha_g = 5$ (dashed–dotted–dotted), $\alpha_g = 5.2$ (dashed–dotted), $\alpha_g = 5.5$ (solid and dashed for unstable), where A and B are fold bifurcation points. Other parameters are $\gamma^{-1} = 0.5$ ps, $\gamma_g^{-1} = 500$ ps, $\gamma_q^{-1} = 10$ ps, $q_0^{-1} = 5.56$ ps, $\alpha_q = 1$.

point are shown in Fig. 2(b) by black and red lines for the gain currents of 209 and 210 mA, respectively.

For our numerical analysis, we chose the parameters of model Eqs. (1)–(3) to match those of a 10 GHz laser [5]: $\tau = 100$ ps, $\gamma^{-1} = 0.5$ ps, $\gamma_g^{-1} = 500$ ps, $\gamma_q^{-1} = 10$ ps, $q_0^{-1} = 5.56$ ps, $\alpha_q = 1$, $\kappa = 0.3$, $s = 10$, and $\xi = 0.05$.

It has been previously noted that strong phase-amplitude coupling in the gain and absorber sections can be linked to complex dynamical behavior of semiconductor lasers [12]. This strong coupling can be accounted for by assuming that the difference between linewidth enhancement factors $\alpha_g - \alpha_q$ in the gain and absorber sections is sufficiently large [5]. In Fig. 3, we chose the pumping parameter g_0 as the continuation parameter to obtain bifurcation diagrams with the help of the DDE-BIFTOOL package [13]. In our numerical simulations, we do not observe Q-switching instability of mode-locked regime. Furthermore, for low values of the linewidth enhancement factor $1 \le \alpha_g < 4.5$, a single branch of fundamental mode-locking solution remains stable, whereas for higher α_g, more branches of stable fundamental mode-locking

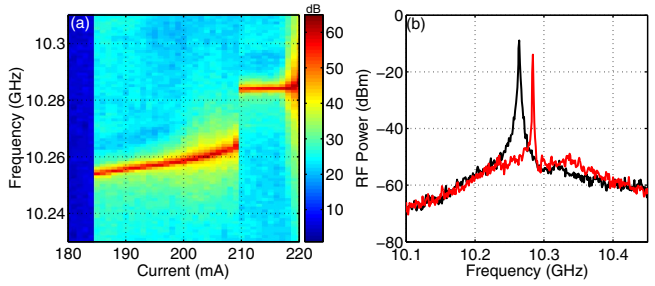

Fig. 2. (a) Evolution of the RF spectrum with gain, laser P_3. (b) RF spectra for the transition point for the gain current of 209 mA (black, left peak) and 210 mA (red, right peak).

can be observed near the lasing threshold. The timing jitter was estimated using Eq. (7) by implementing a MATLAB code for calculation of the eigenfunctions of the adjoint eigenproblem (5). We find that a bistability between two mode-locked regimes exists in the model (1)–(3) for g_0 between 6.048 and 6.05 ns^{-1}, see Fig. 3(a). We see from Fig. 3(b) that for each of the two branches the timing jitter first decreases with increasing g_0 and then increases toward the instability threshold of the mode-locking regime. Similarly to the experimental results of Fig. 2, timing jitter drops abruptly when the solution switches from the branch staring at the point A to the branch starting at the point B. When the linewidth enhancement factor α_g is decreased to 5.2, the fold bifurcations disappear, see dash-dotted line in Fig. 3(a), and a single branch of mode-locking regime remains stable. However, as it is illustrated by the dash-dotted line in Fig. 3(b), the pulse timing jitter dependence on the pump parameter remains similar to that in the bistable case, demonstrating large peaks near the former instability points. These peaks become smaller for lower $\alpha_g = 5$. Our simulations performed with the help of the software package DDE-BIFTOOL indicate that the peaks of timing jitter appear when one of the negative Lyapunov exponents of the mode-locked solution $\psi_0(t)$ comes close to zero with the change of the parameter g_0. Such local increase in the pulse timing jitter obtained numerically is in agreement with the experimental results shown in Fig. 1(b) for the laser P_2. Finally, for sufficiently small $\alpha_g = 3.7$, we observe monotonous decrease of the pulse timing jitter with the increase of g_0, which is in agreement with the experimental data of [9] and the data obtained with the laser P1, see Fig. 1(b).

In conclusion, we have studied theoretically and experimentally the effect of noise on the characteristics

of a two-section semiconductor laser operating in fundamental mode-locking regime. We have proposed a semi-analytical method for estimation of timing jitter in a system of DDEs (1)–(3) describing this laser. The proposed method can be applied to study noise characteristics of other multimode laser devices modeled by systems of delay-differential equations [11,15,21,22]. Using the software package DDE-BIFTOOL, we have studied the dependence of the timing jitter on the injection current and other laser parameters and, in contrast to previous theoretical results [9], we have demonstrated that this dependence can be nonmonotonous. Specifically, we have observed a peak in the gain dependence curve of timing jitter, which is related to the presence of a real Lyapunov exponent approaching zero from below. Our results suggest that in the bistable regime of operation the branch of mode-locking regime that is stable at lower injection currents exhibits higher level of pulse timing jitter. A sudden drop in the timing jitter is observed when the laser switches to another branch of mode-locking regime with the increase of the current.

A. P. and A. G. V. acknowledge the support of SFB 787 of the DFG, project B5, and of the grant 14-41-00044 of RFS. T. H. acknowledges the support of EU FP7 IEF HARMOFIRE project, Grant No. 299288 and IRC Government of Ireland postdoctoral fellowship, grant GOIPD/2014/228 (TUSELAMO). G. H., S. P. H. and A. G. V. acknowledge the support of EU FP7 ITN PROPHET, Grant No. 264687. A. G. V. and G. H. acknowledge the support of SFI E. T. S. Walton Visitors Award, grant 11/W.1/I2073. G. H. and S. P. H. were also supported by the SFI under Contract No. 11/PI/1152, and under the framework of the HEA PRTLI Cycle 5 Structured Ph.D. Programme INSPIRE. D. R. acknowledges the support of NSF grant DMS1413223.

References

1. P. J. Delfyett, S. Gee, M.-T. Choi, H. Izadpanah, W. Lee, S. Ozharar, F. Quinlan, and T. Yilmaz, J. Lightwave Technol. **24**, 27012719 (2006).
2. M. Costa e Silva, A. Lagrost, L. Bramerie, M. Gay, P. Besnard, M. Joindot, J.-C. Simon, A. Shen, and G.-H. Duan, J. Lightwave Technol. **29**, 609 (2011).
3. L. A. Jiang, M. E. Grein, E. P. Ippen, C. McNeilage, J. Searls, and H. Yokoyama, Opt. Lett. **27**, 49 (2002).
4. C.-Y. Lin, F. Grillot, Y. Li, R. Raghunathan, and L. F. Lester, Opt. Express **18**, 21932 (2010).
5. A. Pimenov, E. A. Viktorov, S. P. Hegarty, T. Habruseva, G. Huyet, D. Rachinskii, and A. G. Vladimirov, Phys. Rev. E **89**, 052903 (2014).
6. K. Silverman, M. Feng, R. Mirin, and S. Cundiff, in *Quantum Dot Devices*, Vol. **13** of Lecture Notes in Nanoscale Science and Technology (Springer-Verlag, 2012), pp. 23–48.
7. H. A. Haus and A. Mecozzi, IEEE J. Quantum Electron. **29**, 983 (1993).
8. L. Jiang, M. E. Grein, H. A. Haus, and E. P. Ippen, IEEE J. Sel. Top. Quantum Electron. **7**, 159 (2001).
9. B. Zhu, I. H. White, R. V. Penty, A. Wonfor, E. Lach, and H. D. Summers, IEEE J. Quantum Electron. **33**, 1216 (1997).
10. J. Mulet and J. Mork, IEEE J. Quantum Electron. **42**, 249 (2006).
11. C. Otto, K. Lüdge, A. G. Vladimirov, M. Wolfrum, and E. Schöll, New J. Phys. **14**, 113033 (2012).
12. A. G. Vladimirov and D. Turaev, Phys. Rev. A **72**, 033808 (2005).
13. K. Engelborghs, T. Luzyanina, and G. Samaey, "DDE-BIFTOOL v. 2.00: a Matlab package for bifurcation analysis of delay differential equations," Technical Report TW-330 (K.U. Leuven, 2001).
14. D. Bimberg and U. W. Pohl, Mater. Today **14**(9), 388 (2011).
15. R. Arkhipov, A. Pimenov, M. Radziunas, D. Rachinskii, A. G. Vladimirov, D. Arsenijevic, H. Schmeckebier, and D. Bimberg, IEEE J. Sel. Top. Quantum. Electron. **99**, 1100208 (2013).
16. S. Guo and J. Wu, *Bifurcation Theory of Functional Differential Equations* (Springer, 2013), p. 49.
17. J. Hale, *Theory of Functional Differential Equations* (Springer-Verlag, 1977), pp. 199–202.
18. T. Habruseva, N. Rebrova, S. P. Hegarty, and G. Huyet, in *Quantum Dot Devices*, Vol. 13 of Lecture Notes in Nanoscale Science and Technology (Springer-Verlag, 2012), pp. 65–91.
19. D. von der Linde, Appl. Phys. B **39**, 201 (1988).
20. F. Kéfélian, S. O'Donoghue, M. T. Todaro, J. G. McInerney, and G. Huyet, IEEE Photon. Technol. Lett. **20**, 1405 (2008).
21. N. Rebrova, G. Huyet, D. Rachinskii, and A. G. Vladimirov, Phys. Rev. E **83**, 066202 (2011).
22. A. Pimenov, V. Z. Tronciu, U. Bandelow, and A. G. Vladimirov, J. Opt. Soc. Am. B **30**, 1606 (2013).